Science Advances

AAAS

advances.sciencemag.org/cgi/content/full/3/5/e1700014/DC1

Supplementary Materials for

How and when does an anticancer drug leave its binding site?

Pratyush Tiwary, Jagannath Mondal, B. J. Berne

Published 31 May 2017, *Sci. Adv.* **3**, e1700014 (2017)
DOI: 10.1126/sciadv.1700014

This PDF file includes:

Reliability of time scales

In fig. S1 we provide the Poisson fits to the distribution of escape times from each of the stable intermediates as described in the main text, as well as for the full overall unbinding times the 12 independent runs. In table S1 we give the associated p-values as quantified through the Kolmogorov-Smirnov test proposed in Ref. *22*, which are all above the recommended threshold of 0.05, showing that the CVs *d* and *w* do a reliable job of capturing the slow dynamics of the system, and that the requirements of Refs. *1–2* have been met.

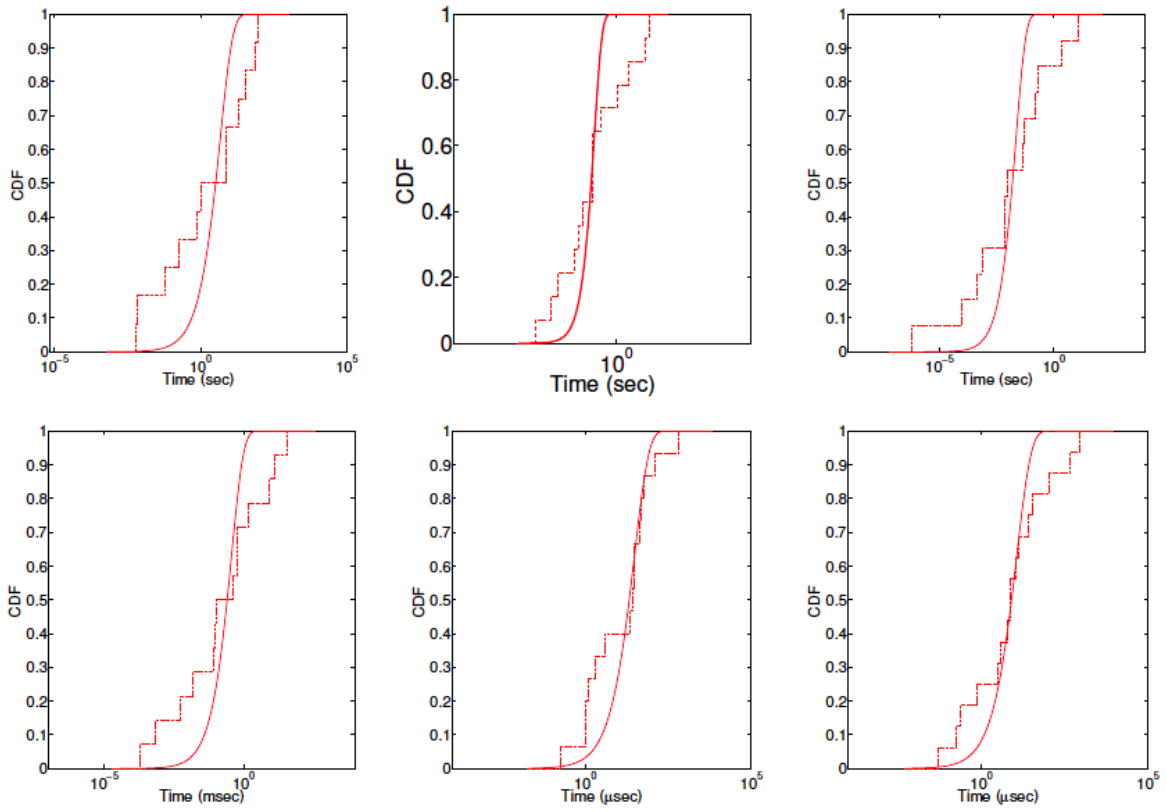

fig. S1. Empirical (dashed line) and fitted cumulative distribution functions (solid line). The p-values for these as per the KS test of Ref. *22* are provided in table S1. From top left to bottom right, these figures correspond to the full unbinding statistics, states 1, 2, 3, 4 and 5.

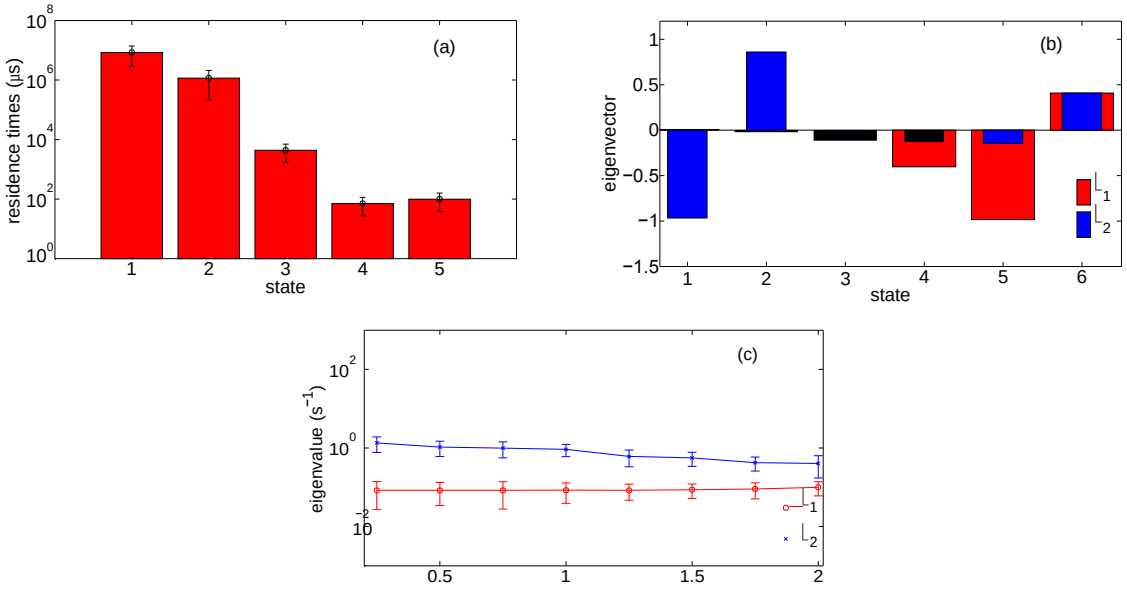

fig. S2. Residence time, eigenvector, and eigenvalue analysis. (**a**) Residence times in various stable states along with standard errors as measured from our simulations. (**b**) and (**c**) Dominant eigenmodes and eigenvalues respectively corresponding to slowest step (red) and second-slowest step (blue). In (b), the change in signs between two states corresponds to movement between them. In (c) the corresponding eigenvalues along with standard errors are plotted as a function of the commitment time in order to demonstrate robustness, i.e. the MD simulation time which the trajectory must spend in a given state before being labeled committed to state. See the section Results in main text for detailed descriptions of the stable states and the eigenmodes

table S1. Residence times and *P* values for various states.

State	Residence time	p-value
Full unbinding	20.7 ± 9.7 sec	0.14
1	8.4 ± 5.5 sec	0.17
2	1.2 ± 0.9 sec	0.13
3	4.4 ± 2.7 msec	0.23
4	70.9 ± 43.6 μsec	0.16
5	99.5 ± 60.6 μsec	0.45

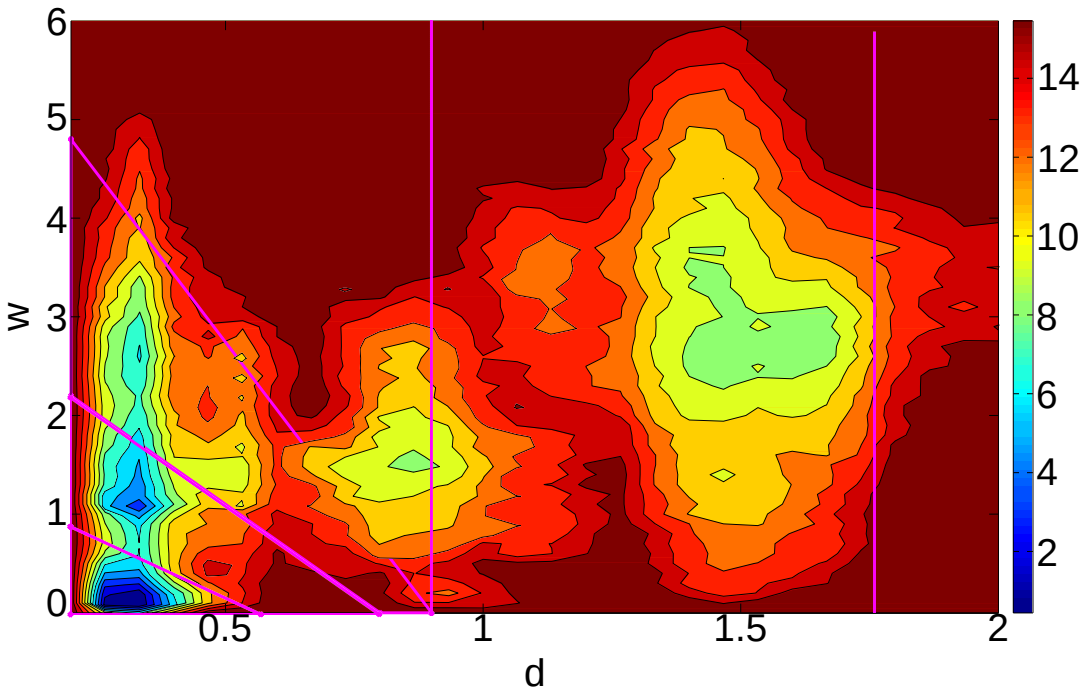

fig. S3. FES as a function of ligand-binding pocket distance *d* (in nanometers) and hydration state of binding pocket *w* calculated using the second set of force fields. Energy is in units of kcal/mol with contours drawn every 0.5 kcal/mol. For reference, we have overlaid the basin classification corresponding used for the first force-field showing rough agreement with the location of stable states here, especially for the initial pocket hydration part with stationary ligand.

Master equation

We set up a master equation for the unbinding dynamics, with absorbing boundary conditions in the state 6 (unbound state). To obtain the state-to-state transition probabilities k_{ij} from state i to j, we use $k_{ij} = \frac{N_{ij}}{t_i}$ for $i = j$, where N_{ij} is the number of observed transitions from state i to j and t_i is the total time spent in state i. k_{ii} is obtained by setting $\Sigma_j k_{ij} = 0$. The full matrix $K = [k_{ij}]$ is provided in table S2. By solving for the slowest eigenvalues of the transition probability matrix K, we get an estimate of the rate-determining steps in the full unbinding dynamics reported in the main text.

In fig. S2(a) and in table S1 we provide the residence time in each state along with associated error bars. Figure S2(b) shows the corresponding eigenvectors that encode information

table S2. Matrix *K* of state-to-state transition rates. All rates are in sec^{-1}.

from (row) - to (column)	1	2	3	4	5	6
1	-0.1191	0.0596	0.0340	0.0170	0.0085	0
2	0.1328	-0.8633	0.5313	0.0664	0.1328	0
3	0	81.5477	-228.3334	146.7858	0	0
4	0	0.0941×10^4	0.0941×10^4	-1.4110×10^4	1.2229×10^4	0
5	0	0	0.0628×10^4	0.1885×10^4	-1.0051×10^4	0.7538×10^4
6	0	0	0	0	0	0

about the slowest and second slowest rate-limiting slow steps in moving between these states. These can be seen by noting the states between which the respective eigenvector changes its sign, indicating movement from one region to another. The physical mechanisms associated with these steps been detailed in the main text. In fig. S2(c) we provide the corresponding eigenvalues λ of the matrix K. While counting transition rates to build a master equation, one ought to be careful of the spurious friction-induced recrossings of the barriers between any two stable states. As such we use a minimum commitment time criterion (in units of MD simulation time) which the trajectory must spend in a given state before being labeled committed to state. Figure. S2(c) shows that the calculated timescales are well converged with respect to the choice of this metric and thus the master equation is robust with respect to treatment of trajectories that display quick recrossings of the transition regions.

Effect of force field

In order to ascertain at least a qualitative robustness of the proposed mechanism in this work with respect to choice of force-field, we repeated 3 calculations with AMBER all-atom force-field and TIP4P water model, the parameters for which were earlier provided in the section “System Specifications”. The objective in repeating the calculation with the newer forcefield was not to obtain converged rate constants but to see if the new force field also gives the water assisted molecular switch mechanism as the route to unbinding. From these we reassuringly find that the molecular switch mechanism reported in this work is not a force-field artifact, and for this force-field as well the unbinding involves αC helix rotation through

Glu46-Lys36 salt bridge breaking, in conjunction with the entry of water molecules. The free energy so obtained through the use of Eq. 4 in main text and averaging the probabilities over the 3 runs is given in fig. S3. In this figure, the basins corresponding to the classification used for the first force-field are also overlaid showing rough agreement. While we do not claim either of the free energy surfaces in this work is converged in terms of relative stabilities of the basins, the agreement with the free energy reported in main text in terms of location of metastable states is satisfactory. The agreement is especially pronounced in the initial binding pocket hydration step, while there are differences in the high energy regions which is not surprising given different protein force-fields and ligand parameterizations. Overall we find mandatory (a) movement through different binding pocket hydration states with the ligand stationary, and (b) the rotation of the αC helix irrespective of force-field choice.